Dynamics of Coulomb fission

Hans Kruse, W. T. Pinkston,* and Walter Greiner
Institut für Theoretische Physik, Johann Wolfgang Goethe-Universität, 6000 Frankfurt am Main, West Germany

Volker Oberacker
Physics Division, Oak Ridge National Laboratory, Oak Ridge, Tennessee 37830

(Received 21 March 1980)

A general formalism is described for the treatment of Coulomb fission, within the framework of the semiquantal theory. We develop a model for the fission probabilities of levels excited in Coulomb excitation. This model contains penetration of the double-humped fission barrier, competition from gamma and neutron emission, and the spreading of the collective states into noncollective compound states. For $^{184}_{74}W+^{238}_{92}U$, the fission probability at $\theta_{c.m.}=180°$ is increased by a factor of 3.9, 3.3, and 2.0 at $E/E_{Coul}=0.77$, 0.85, and 0.935, respectively, compared to the simplified sharp cutoff model used in earlier model calculations. The enhancement comes from barrier penetration. The damping of the fission probability due to spreading into noncollective compound states is small. Prompt Coulomb fission (near the distance of closest approach) is studied in a one-dimensional model. The results clearly imply that prompt fission is negligible. We have also studied the sudden approximation for collective rotational levels in connection with Coulomb fission. At high spins ($I\approx 20$), it leads to significant errors. Contrary to the basic assumption of the sudden approximation that the nuclear symmetry axis remains fixed during the collision, it is shown that Coulomb excitation results in a strong alignment of the nuclear symmetry axis perpendicular to the beam axis at small internuclear distances.

[NUCLEAR REACTIONS, FISSION Semiquantal theory of prompt and asymptotic Coulomb fission, study of double-humped barrier penetration, damping effects, neutron and γ emission. Calculated $\sigma(E_p, \theta_{c.m.}=180°)$.]

I. INTRODUCTION

In anticipation of modern heavy-ion accelerators, Guth and Wilets[1] proposed experiments to observe *Coulomb fission* (CF), a new kind of process induced entirely by the strong time-varying electric interaction between heavy-ion projectile and target nucleus. Coulomb fission is unique among fission mechanisms in that the Coulomb interaction couples directly to the collective fission degree of freedom. All other fission mechanisms proceed indirectly through noncollective, compound nuclear states. As a result, CF should be faster than other fission processes. Since the Coulomb interaction with collective modes is rather well understood, CF should be an excellent probe for investigating collective potential energy surfaces and collective dynamics at high excitation energy and large deformations.

A number[2-8] of theoretical calculations of CF have been published. These calculations confirm the above conjecture, viz., that CF should be a sensitive probe. Because of differences in the treatment of reaction dynamics and of nuclear structure in these calculations, their predictions differ significantly. Predictions of cross section magnitudes differ by as much as 3 orders of magnitude. Different assumptions lead to predictions of angular distributions which are qualitatively different.

Experimentally,[9] CF has been observed only recently, and its characteristics are still not well known. Sub-Coulomb, heavy-ion induced fission events, suggestive of CF, had been observed earlier at Berkeley[10,11] and at GSI[12,13]; however, in those experiments it was impossible to separate CF events from fission induced by the transfer of one or more neutrons.

At sub-Coulomb energies, all the available data seem to agree rather well with the predictions based on the approach of Oberacker *et al.*[5] The experimental results of Backe *et al.*[9] for the CF of ^{238}U induced by bombardment with W ions are shown in Fig. 1, along with the theoretical predictions of Oberacker.[14] Results consistent with the earlier Berkeley and GSI data were discussed in Ref. 8. There is no experimental evidence for the deep Coulomb-nuclear interference minimum predicted by the theory. This interference seems to depend sensitively on the nature of the nuclear interaction of the ions at short distances and is under study.

Because of the success of our approach in the sub-Coulomb region, and because of the large discrepancies between the predictions of competing models, we present here a discussion of the dynamics of CF in order to illuminate the validity and consequences of some of the important assumptions and approximations underlying various ap-

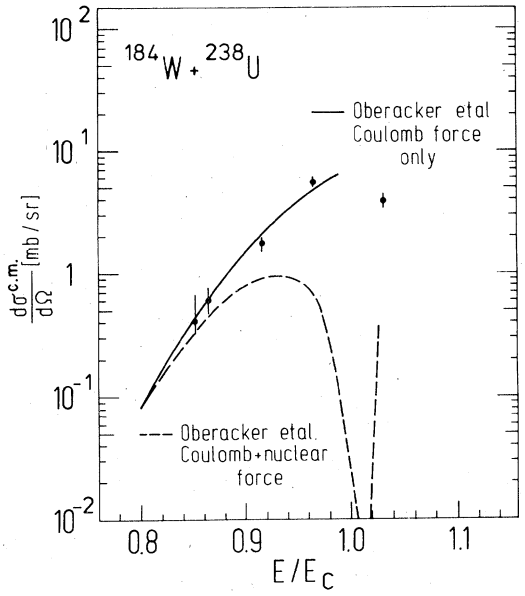

FIG. 1. Experimental observation of Coulomb fission (Ref. 9) compared to the theoretical predictions (Refs. 8 and 14).

proaches. We also discuss the competition of fission with other decay modes and the damping of collective states into noncollective compound states. These have not been treated previously in the literature.

We begin with a brief outline of the coupled-equations approach of Oberacker, Holm, and Greiner,[4,5,8] indicating how earlier calculations can be generalized easily to include coupling of collective bound states to continuum states and to noncollective compound levels. In Sec. III we critically examine the use of the sudden approximation in treating rotational excitations. Section IV is concerned with the justification of the neglect of direct couplings to the continuum in the Coulomb excitation calculations—"prompt fission." Results summarized there are covered in greater detail in the Appendix. In Sec. V, a model of fission probabilities is described which is more realistic than the classical "sharp cutoff" model used earlier.[4,5,8] Numerical results are given.

II. FORMAL TREATMENT

The mechanism of CF is Coulomb excitation of collective resonances followed by spontaneous fission. We study the CF problem in semiquantal approximation and derive a set of coupled equations for fission caused by inelastic Coulomb or nuclear excitation. Let us first consider the total Hamiltonian in the center-of-mass system,

$$H(\xi_p, \xi_t, \vec{r}) = T_{\rm rel} + H_p(\xi_p) + H_t(\xi_t) + \tilde{V}_{pt}(\xi_p, \xi_t, \vec{r}) . \tag{2.1}$$

The first term describes the kinetic energy of relative motion. The symbols ξ_i and H_i $(i=p,t)$ represent the intrinsic coordinates and Hamiltonians of the projectile and target nucleus, respectively. $\tilde{V}_{pt}$ denotes the interaction potential consisting of a real Coulomb and a complex optical potential,[15]

$$\tilde{V}_{pt}(\xi_p, \xi_t, \vec{r}) = V_{\rm Coul} + (V + iW)_{\rm nucl} . \tag{2.2a}$$

This potential may be split up into two parts,

$$\tilde{V}_{pt} = U(\vec{r}) + [\tilde{V}_{pt} - U(\vec{r})] = U + V_{pt} , \tag{2.2b}$$

where $U(\vec{r})$ is the real elastic potential depending upon the relative coordinate only. The second term V_{pt} contains the complex coupling potentials and the elastic imaginary potential. In this paper we consider the excitation and fission of very heavy systems like $^{184}W + ^{238}U$ at bombarding energies $E < 1.05 E_{\rm Coul}$. Under these restrictions we can treat the relative motion of the colliding nuclei classically and neglect the small change in the orbit due to energy and angular momentum transfer caused by the coupling potentials. The classical trajectory is therefore determined by the real elastic potential $U(\vec{r})$,

$$\mu \ddot{\vec{r}}(t) = -\nabla U[\vec{r}(t)] . \tag{2.3}$$

We treat the internal dynamics of the nuclei quantum mechanically. This yields the time-dependent Schrödinger equation,

$$\left[H_p(\xi_p) + H_t(\xi_t) + V_{pt}[\xi_p, \xi_t, \vec{r}(t)] - i\hbar \frac{\partial}{\partial t}\right] \psi(\xi_p, \xi_t, t) = 0 . \tag{2.4}$$

If we restrict ourselves to the dominant monopole-multipole interaction,[16] i.e.,

$$V_{pt}[\xi_p, \xi_t, \vec{r}(t)] = V_p[\xi_p, \vec{r}(t)] + V_t[\xi_t, \vec{r}(t)] , \tag{2.5}$$

the Schrödinger equation separates into two equations depending upon the internal coordinates of either nucleus only. These have the form

$$\left\{H(\xi) + V[\xi, \vec{r}(t)] - i\hbar \frac{\partial}{\partial t}\right\} \psi(\xi, t) = 0 . \tag{2.6}$$

Since an exact solution of Eq. (2.6) is not possible (except in oversimplified, one-dimensional cases in which the differential equation can be solved numerically), approximations must be made. Two approaches have been put forward, both based on the collective model. Levit and Smilansky apply a semiclassical theory based on the path-integral formalism. All other authors expand $\psi(\xi, t)$ in a finite set of collective bound state wave functions, then solve the resulting coupled system of ordinary differential equations for the time-dependent amplitudes. We shall in this section follow the latter philosophy, generalizing the method to in-

clude couplings to the continuum and noncollective bound states. We begin with a review of the Oberacker-Holm-Greiner (OHG) approach.

A. The Oberacker-Holm-Greiner model

The coupled equations approach follows from the expansion of ψ:

$$\psi = \sum_{\mu} \varphi_{\mu} e^{-i\omega_{\mu} t} a_{\mu}(t) , \tag{2.7}$$

in which $\{\varphi_{\mu}\}$ is a set of collective model wave functions with energies $\{\epsilon_{\mu} = \hbar\omega_{\mu}\}$. In the OHG calculations, the rotation-vibration model (RVM)[17] is used. The internal variables ξ are the deformation coordinates a_{20}, a_{22}, and the Euler angles, θ_i. Oberacker *et al.*[5,8] used a basis of order 256 consisting of rotational bands built upon beta and gamma vibrations. Substitution of Eq. (2.7) into Eq. (2.6) results in

$$i\hbar\dot{a}_{\mu} = \sum_{\nu} a_{\nu}(t) \langle \varphi_{\mu} | V(t) | \varphi_{\nu} \rangle e^{i(\omega_{\mu} - \omega_{\nu})t} . \tag{2.8}$$

This system is solved as a function of time. A typical result of such calculations is sketched in Fig. 2 for a highly excited level. The probability $|a_{\mu}|^2$ rises quickly after $t = 0$ to its asymptotic value $|a_{\mu}(\infty)|^2$. Because of the rapid rise of $|a_{\mu}|^2$, one can think of CF as proceeding in two stages, Coulomb excitation followed by decay. The CF cross section is given by

$$\sigma_{CF} = \sigma_R \sum_{\mu} |a_{\mu}(\infty)|^2 p_{\mu} . \tag{2.9}$$

In Eq. (2.9), σ_R is the Rutherford cross section, and p_{μ} is the branching ratio

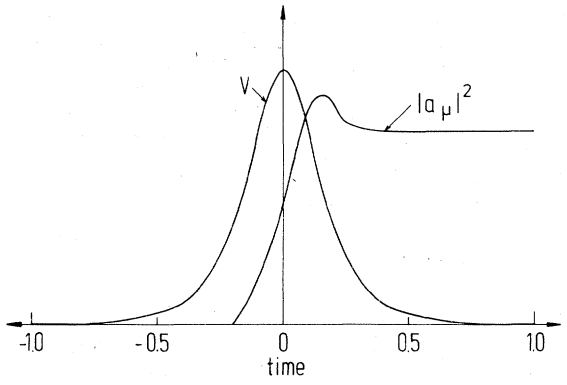

FIG. 2. A sketch of the amplitude squared $|a_{\mu}|^2$ for a typical fissioning level, and of the strength of the monopole-quadrupole part of the Coulomb potential as function of the time. The time of closest approach on the Rutherford trajectory is $t = 0$. The unit of time in the sketch is the period of beta vibrations, $2\pi\hbar/E_{\beta}$.

$$p_{\mu} = \frac{\Gamma_{\mu f}}{\Gamma_{\mu f} + \Gamma_{\mu \gamma} + \Gamma_{\mu n} + \cdots} . \tag{2.10}$$

A simplified version of Eq. (2.10) has been used by Holm and Greiner[4] and by Oberacker *et al.*[5,8] This recipe is based on barrier penetration considerations. The penetrability of a barrier varies extremely rapidly with energy near the barrier top, changing from very nearly zero to nearly one as the energy rises above the barrier top. Based on these qualitative considerations, a classical or sharp cutoff model is introduced, in which $p_{\mu} = 0$, $\epsilon_{\mu} < B$; $p_{\mu} = 1$, $\epsilon_{\mu} > B$, where B is the height of the fission barrier. Barrier parameters are taken from analyses[18] of (d,p), (t,p) induced fission. Despite the success of the calculations of Oberacker *et al.* in correctly predicting experimental results, this primitive model of the fission probabilities clearly requires further study and justification. Because barrier penetration is ignored, the results may be overly sensitive to barrier parameters. Barrier parameters are obtained from experimental data but are model dependent; different theoretical models result in slightly different parameter sets. The OHG approach should also be refined to include the spreading of the collective states into background compound states. This step is necessary for the correct treatment of competing processes, such as gamma ray/neutron emission, since these processes result primarily from the decay of the compound states.

Before generalizing the OHG approach in these ways, we comment on a closely related point arising from a criticism by Levit and Smilansky[6] of the OHG theory. These authors question the validity of replacing unbound states, near the barrier top and above, by discrete levels. Although this is a legitimate concern, the problem is a quantitative rather than a qualitative one. Certainly one can and constantly does represent states in the continuum quite accurately by bound states. *All* heavy nuclei undergo spontaneous fission; therefore all their states including their ground states are actually resonances in the scattering of fission fragments. For low-lying states, these resonances are extremely narrow, which implies that the "on-resonance" continuum wave functions are much larger inside the nucleus than outside. Also, the wave functions inside the nucleus undergo negligible changes in shape as the energy changes across the resonance. As a result, the interior parts of the wave functions can be replaced accurately by bound states with normalizations which are energy dependent. Transition probabilities for transitions between resonant states, integrated over energies, agree extremely well with transi-

tion probabilities calculated with bound wave functions. In such a region of sharp resonances, the wave functions of states off resonance are negligible in the interior; thus in Coulomb excitation calculations the coupling between these states and resonant states can be neglected. Near the barrier top and above it, the resonances become wider and then begin to overlap. The distinction between resonant and nonresonant becomes hazy, and the validity of calculations based on bound wave functions becomes less obvious. However, past experience (e.g., giant multipole resonances) indicates that bound state methods are often surprisingly accurate even when the resonances are quite broad. In the next section we generalize the OHG model to include couplings to the continuum. We assume that the results derived there can be applied to Coulomb fission even though we can easily establish their validity only for narrow states.

B. An exact system of coupled equations

The basis of the previous section can be expanded to include continuum states and also noncollective bound states. We denote these states by φ_E and φ_K, respectively. We use Greek indices for collective bound states, Latin indices for compound states, and denote continuum states by the energy variable E. The φ_μ and φ_K states are truly bound (normalizable). If H denotes the exact Hamiltonian, these states are eigenstates of the zero order Hamiltonian, i.e.,

$$H_0 = \sum_\mu P_\mu H P_\mu + \sum_K P_K H P_K + QHQ\,,$$
$$Q = 1 - \sum_\mu P_\mu - \sum_K P_K\,. \tag{2.11}$$

In Eq. (6), the P and Q operators are projectors, e.g., $P_\mu = |\varphi_\mu\rangle\langle\varphi_\mu|$. If the φ_μ are properly chosen, the continuum states φ_E will be nonresonant. We assume delta function normalization of the φ_E, i.e.,

$$\langle\varphi_E|\varphi_{\bar{E}}\rangle = \delta(E-\bar{E})\,.$$

The collective states couple to the continuum with escape widths,

$$\Gamma_{\mu f} = 2\pi|\langle\varphi_\mu|H|\varphi_E\rangle|^2 \equiv 2\pi|H_{\mu E}|^2\,. \tag{2.12}$$

We assume that the escape widths of the noncollective states φ_K are negligible, so that the collective states are "doorways" to fission. We further assume that the Coulomb excitation preferentially connects collective states, so that

$$\langle\varphi_K|V|\varphi_I\rangle \equiv V_{KI} = 0 = \langle\varphi_K|V|\varphi_\mu\rangle \equiv V_{K\mu} = 0 = V_{KE}\,.$$

Coulomb fission is unique among fission mechanisms in that the doorway is directly excited.

In Ref. 8, the coupling to compound states was neglected. The prompt fission couplings $\langle\varphi_\mu|V|\varphi_E\rangle$ were also neglected. The resulting coupled equations are written down there. It was argued, based on what is observed in Fig. 2, that CF is a two-step process, so that the coupled equations for Coulomb excitation can be solved first, neglecting continuum couplings. Then, at later times when $V(t)\approx 0$, the decay into the continuum can be solved for the fission width, Eq. (2.12).

A more economical procedure, which avoids the need for two separate steps, is to work directly in the continuum basis. We use as our basis the exact eigenstates of H. These new states have the form

$$\chi_E^{(\mu)} \simeq A_\mu(E)\varphi_\mu + \sum_K B_{\mu K}(E)\varphi_K + \int dE' C_\mu(E,E')\varphi'_K\,. \tag{2.13}$$

The coefficients A, B, and C in Eq. (2.13) can be determined, formally at least, by the approach of Fano.[19] Clearly, Eq. (2.13) is not completely general. In writing it, we assume that, to a good approximation, the strength of a collective state φ_μ is spread over a small energy region in the neighborhood of ϵ_μ. No χ_E state has admixed in it more than one collective component. These assumptions are not valid for strongly damped states.

The φ_μ states are strongly excited in Coulomb excitation, and they decay strongly due to their coupling to the φ_E states. This coupling results in an "escape width." Their coupling to the φ_K also results in a spreading of the strength over energy. In addition, the φ_K are strongly coupled to other continua, not included in our formalism. These couplings correspond to gamma-ray and neutron emission and result in a decrease of fission probabilities. The effect of these competing processes on the fission probability will be discussed in detail in Sec. V.

We assume that the wave function ψ can be expanded as

$$\psi = \sum_\mu \int dE\, a_{\mu E}(t)\chi_E^{(\mu)} e^{-iEt/\hbar}\,. \tag{2.14}$$

In Eq. (2.14) we assume that each of the energy integrations covers a finite energy range about ϵ_μ. Substitution into Eq. (2.6) results in coupled equations of the form

$$i\hbar\dot{a}_{\mu E} e^{-i\omega_{\mu E}t} = \sum_\nu \int d\bar{E} a_{\nu\bar{E}} e^{-i\omega_{\nu\bar{E}}t}\langle\chi_E^{(\mu)}|V|\chi_{\bar{E}}^{(\nu)}\rangle\,. \tag{2.15}$$

We assume that $\langle\varphi_E|V|\varphi_\mu\rangle$ can be neglected in

Eq. (2.15). This means we neglect the direct excitation of the continuum. In an energy region of very narrow resonances, we know this is a good approximation, as discussed earlier. Because these neglected matrix elements are important only during the collision time, we consider them to be the source of prompt fission events, as opposed to the "asymptotic fission" resulting from the radioactive decay of quasibound collective states. Prompt fission will be considered further in Sec. IV.

If the matrix elements $\langle\varphi_E|V|\varphi_\mu\rangle$ can be neglected, then Eq. (2.15) can be simplified as follows:

$$i\hbar\dot{a}_{\mu E}e^{-i\omega_{\mu E}t} = A_\mu(E)^* \sum_\nu V_{\mu\nu}(t) \times \int d\bar{E}\, A_\nu(\bar{E})e^{-i\omega_{\nu\bar{E}}t}a_{\nu\bar{E}}\,. \tag{2.16}$$

This can be rewritten in the following form:

$$i\hbar\dot{a}_{\mu E}e^{-i\omega_\mu t} = A_\mu(E)^* \sum_\nu V_{\mu\nu}(t)e^{-i\omega_\nu t} \times \int d\bar{E}\, A_\nu(\bar{E})a_{\nu\bar{E}}e^{i[(\omega_{\mu E}-\omega_\mu)t-(\omega_{\nu E}-\omega_\nu)t]}\,. \tag{2.16'}$$

If the exponential factor in the integral on the right of Eq. (2.16′) can be approximated by unity, then the resulting approximate system has as its solution

$$a_{\mu E} = a_\mu(t)A_\mu(E)^*\,, \tag{2.17}$$

in which $a_\mu(t)$ is a solution of Eq. (2.8). In this approximation, the effect of spreading on Coulomb excitation is to spread the probability $|a_\mu|^2$ over a sharply peaked distribution centered about ϵ_μ. Neglecting the variation of the exponential with time is justified if the collision time is sufficiently short. Using Γ_μ, Γ_ν as measures of $|\omega_{\mu E}-\omega_\mu|$, $|\omega_{\nu\bar{E}}-\omega_\nu|$, then the validity criterion is

$$\tau \ll \pi\hbar/\Gamma\,, \tag{2.18}$$

in which τ is the time interval over which $|V_{\mu\nu}A_\nu|$ is non-negligible and Γ represents Γ_μ or Γ_ν. From the sketch in Fig. 2, one sees that this product is of the order of half the collision time. A collision time is typically half a period of beta vibration; therefore the inequality Eq. (2.18) holds for spreading widths small compared to $2h\omega_\beta$.

The generalization of Eqs. (2.9) and (2.10) follows immediately from this formalism. The fission probability of a state at energy E depends on the ratio of escape widths of the several continua contained in $\chi_E^{(\mu)}$. We can write immediately

$$\sigma_{CF} = \sigma_R \sum_\mu |a_\mu(\infty)|^2 \int dE\,|A_\mu(E)|^2 \times \frac{\Gamma_f(E)}{\Gamma_f(E)+\Gamma_\gamma(E)+\Gamma_n(E)+\cdots}\,. \tag{2.19}$$

Equation (2.19) is the basis of model calculations discussed in Sec. V.

Before proceeding to estimates of the fission probability based on Eq. (2.19), we first discuss two approximations which have been introduced to simplify CF calculations. The first is the use by Beyer and Winther[3] and Levit and Smilansky[6] of the sudden approximation in treating the rotational degrees of freedom. The other is our own neglect of direct couplings to the nonresonant continuum, i.e., prompt fission.

III. THE SUDDEN APPROXIMATION

In the papers of Beyer and Winther[3] and Levit and Smilansky,[6] the excitation of rotational states is treated in sudden approximation. This approximation greatly simplifies the solution of Eq. (2.6) by reducing the number of degrees of freedom of the physical system. However, the results of Ref. 6 are significantly different from those of Ref. 8, especially the angular distributions of fission fragments. Since the sudden approximation was not employed in Ref. 8, we suspect that its use is the source of the discrepancy. Accordingly, in this section we investigate the validity of this use of the sudden approximation.

It is convenient here and in the following section to work with a simple model of an axially symmetric nucleus, capable of rotations and axially symmetric deformations depending upon a single coordinate β. For such a system, Eq. (2.6) becomes

$$\left\{i\hbar\frac{\partial}{\partial t} - H_v(\beta) - T_r(\beta,\theta) - V[\beta,\theta,\vec{r}(t)]\right\}\psi(\beta,\theta,t) = 0\,. \tag{3.1}$$

The rotational kinetic energy is T_r; the Hamiltonian H_v corresponds to vibrations and fission. In the sudden approximation, T_r is neglected during the collision. The result is a one-dimensional time-dependent Schrödinger equation with solutions parametrized by θ. Levit and Smilansky[6] solve the resulting equation approximately by their path integral method; however, its solution to any desired accuracy by numerical procedures is quite feasible. From these solutions the fission yield at each orientation, and thus the angular distribution, can be computed.

A. Comparison with exact calculations

The sudden approximation consists of setting equal to one all the exponential factors on the right side of Eq. (2.8). Its validity[16] depends on the magnitude of the parameter, $\xi = \Delta E \tau_c/\hbar$, in which τ_c is the collision time and $\Delta E/\hbar$ is a measure of the quantities $|\omega_\mu - \omega_\nu|$, which are neglected in Eq. (2.8). Thus the sudden approximation should be valid for $\xi \ll 1$. As we have seen, τ_c is about half a beta vibrational period. In Coulomb fission, states with values of $I = 20$ or more are important. We, therefore, choose for ΔE the difference in energy of the $I = 20$ and $I = 18$ members of the ground-state band in ^{238}U. The resulting ξ value is 0.7; thus the sudden approximation is suspect. These suspicions are easily confirmed by the results of the following calculation. We calculated the Coulomb excitation of a rigid rotor by exact numerical integration of the equation

$$\left[i\hbar\frac{\partial}{\partial t} - T_r(\beta_0,\theta) - \tfrac{1}{2}Z_1\frac{eQ}{r(t)^3}P_2(\cos\theta)\right]Y(\theta,t) = 0\,. \tag{3.2}$$

The charge Z_1 is that of the projectile. The symbol Q represents the intrinsic quadrupole moment of the target nucleus. This parameter and the moment of inertia in the operator, T_r, can be obtained from the energy spacings and $B(E2)$'s in the ground state band of the target. Only collisions of zero impact parameter were treated, so that the azimuthal angle φ can be ignored. The angle θ is the angle between the beam axis and the nuclear symmetry axis. The initial wave function $Y(\theta,-\infty)$ is the spherical harmonic Y_{00}.

In this simple model, the sudden approximation is also quite easily calculated. Neglecting all energy differences in the exponential factors in Eq. (2.8) is mathematically equivalent to neglecting T_r in Eq. (3.2). If this is done, the solution is given by

$$Y_S(\theta,t) = Y_{00}\exp\left[-\frac{i}{\hbar}\int_{-\infty}^{t} V(\theta,t')dt'\right]. \tag{3.3}$$

The integral in Eq. (3.3) can be evaluated analytically, yielding

$$Y_S(\theta,t) = \frac{1}{\sqrt{4\pi}}\exp\left(\frac{-iZ_1Qe}{\hbar^2\eta r_0^{2/3}}(3\cos^2\theta - 1) \times\left\{K(\infty) + K\left[\left(\frac{r(t)}{r_0 - 1}\right)^{1/2}\right]\right\}\right), \tag{3.4}$$

$$\eta = \left(\frac{2Z_1Z_2e^2}{m_{12}}\right)^{1/2},$$

$$K(x) = \tfrac{2}{3}(x^3 + 2x)(x^2 + 1)^{-3/2}.$$

The charge Z_2 is that of the target, r_0 is the distance of closest approach, and m_{12} is the reduced mass of the system.

The resulting asymptotic wave functions $Y(\theta,\infty)$ and $Y_S(\theta,\infty)$ can be expanded, as in Eq. (2.7), in spherical harmonic functions $Y_{I0}(\theta,0)$. This yields the values of the expansion coefficients, $a_I(\infty)$ and $a_I^{(S)}(\infty)$, which are listed in Table I. Two cases were considered: ^{132}Xe on ^{238}U and ^{238}U on ^{238}U. The results are quoted for bombarding energies, expressed as multiples of the Coulomb energy, defined by[11]

$$E_{\text{Coul}} = Z_1Z_2e^2/R, \qquad R = 1.16(A_1^{1/3} + A_2^{1/3} + 2)\ \text{(fm)}. \tag{3.5}$$

From Table I it is clear that the sudden approximation greatly overestimates the population of high angular momentum states. What effect this has on the fission cross sections is not completely clear

TABLE I. Expansion coefficients $|a_J(\infty)|$ for Coulomb excitation of a rigid rotor.

	^{132}Xe–^{238}U at $0.85E_{\text{Coul}}$ $\lvert a_I\rvert$			^{238}U–^{238}U at $0.8E_{\text{Coul}}$		
J	exact	sudden	S/E	exact	sudden	S/E
0	5.88(−2)	3.41(−2)	0.58	6.62(−2)	2.80(−2)	0.42
2	7.30(−2)	2.66(−2)	0.36	7.02(−2)	1.96(−2)	0.28
4	7.55(−2)	6.06(−2)	0.80	8.38(−2)	4.76(−2)	0.57
6	6.44(−2)	1.61(−2)	0.25	5.95(−2)	1.48(−2)	0.25
8	8.89(−2)	7.26(−2)	0.82	8.18(−2)	5.18(−2)	0.63
10	4.22(−2)	3.66(−2)	0.87	4.75(−2)	2.84(−2)	0.60
12	1.07(−1)	2.94(−1)	0.27	8.47(−2)	2.73(−2)	0.32
14	5.85(−2)	1.02(−1)	1.74	3.86(−2)	6.88(−2)	1.78
18	1.37(−1)	1.24(−2)	0.09	6.50(−2)	3.96(−2)	0.61
22	7.62(−2)	1.75(−1)	2.30	9.20(−2)	3.51(−2)	0.38
26	5.15(−3)	8.51(−2)	16.52	6.55(−2)	7.97(−3)	1.22
30	8.35(−5)	1.16(−2)	138.90	4.68(−3)	1.41(−2)	30.13

to us, but we suspect that the use of the sudden approximation overestimates the fission cross section by giving too large a probability to high spin states near the barrier top and above. Another important angular momentum effect, neglected by Levit and Smilansky, is the lowering of the effective fission barrier due to centrifugal stretching. It is very clear that the use of the sudden approximation will lead to significant errors in the angular distribution of fission fragments, since the angular distribution depends upon the relative population of different angular momentum states.

Further insight into the shortcomings of the sudden approximation can be obtained by inspection of the wave function $Y(\theta,t)$ plotted in Fig. 3. What is plotted is actually $\sin\theta\,|Y(\theta,t)|^2$; the quantity $2\pi|Y(\theta,t)|^2\sin\theta d\theta$ is the probability of observing the rotor with orientation within $d\theta$ about θ. The curves are labeled by distances between projectile and target; negative distances correspond to the ingoing branch of the Rutherford trajectory; positive distances correspond to the outgoing branch. The case illustrated is ^{238}U-^{238}U at $E=0.8E_c$. One sees that the idea that the orientation of the target is fixed during the collision is quite wrong. What actually happens is that the Coulomb field exerts a torque which strongly aligns the nuclear symmetry axis perpendicular to the beam direction. The maximum alignment occurs shortly after closest approach, $r\approx 25$ fm, the delay being an inertial effect. At much later times the alignment disappears and $|Y(\theta,t)|^2$ oscillates rapidly. If CF is prompt, occurring during τ_c, then it is clear from Fig. 3 that the fission fragments distribution

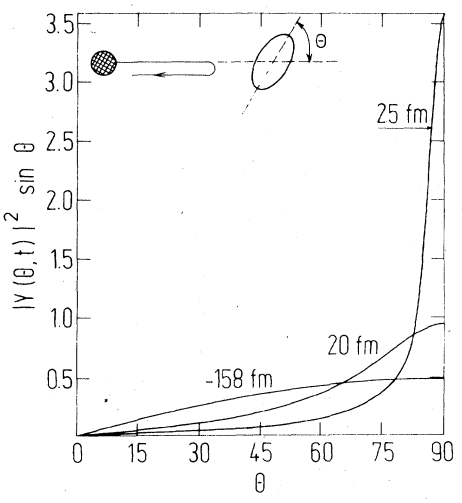

FIG. 3. Probability density as a function of the angle θ for a ^{238}U-^{238}U collision in which the nuclei are treated as rigid rotors. The curves are labeled by r, the distance along the Rutherford trajectory. A negative r implies the ingoing branch of the Rutherford trajectory.

should be sharply peaked at 90° relative to the beam. We conclude that the sudden approximation is invalid for CF calculations. However, none of the results discussed above contradicts the well-known result[16] that the sudden approximation is valid for the excitation of low-lying rotational states in lower energy collisions or collisions with much lighter ions. In such cases, the relevant value of ΔE is the 0^+-2^+ energy spacing in the ground band. This choice results in ξ values of order 0.1.

B. Comparison with classical mechanics

Although the sudden approximation is not a semiclassical approximation, classical arguments are often put forward to justify the sudden approximation. The sudden approximation assumes that the angle θ can be kept fixed during a collision. Classical calculations predict that aligning torques produce rotations of only a few degrees, in agreement with θ being approximately fixed.

The results plotted in Fig. 3 contradict the predictions of classical mechanics. The classical quantity analogous to that plotted in Fig. 3 is the distribution function of an ensemble of identical systems, with random orientation initially. Since the classical torques produce very small rotations, the distribution function of a classical system will change very little, during a collision, from its initial isotropic form. However, classical mechanics is not a good approximation to these processes, which is illustrated by yet another calculation.

In order for classical mechanics to be valid it must be possible to form a narrow wave packet which does not spread appreciably during the process of interest. Accordingly, we solved Eq. (3.2) with the interaction term V set to zero. An initial wave function was chosen consisting of a Gauss packet with a width of about 10° about the forward direction, $\theta=0$. (Since there is no external field, all angles are equivalent, and $\theta=0$ is a convenient choice, since φ can be neglected.) Solutions of Eq. (3.2) are plotted in Fig. 4 at three times, $t=0$, $0.32\tau_\beta$, and $0.95\tau_\beta$. The unit of time τ_β is the period of beta vibrational motion, $\tau_\beta=2\pi/\omega_\beta$, $\hbar\omega_\omega\simeq 1$ MeV. A collision time is of order $0.5\tau_\beta$ to $0.6\tau_\beta$. The figure clearly shows significant spreading, due to the uncertainty principle, during a collision time; this invalidates the classical method. (An initial width of 5° would result in a much greater spreading.) The physical reasoning for the spreading is obvious: A narrow packet requires large angular momentum components, which result in large angular displacements.

These results clearly illustrate the incorrectness of a *purely classical* description of the rota-

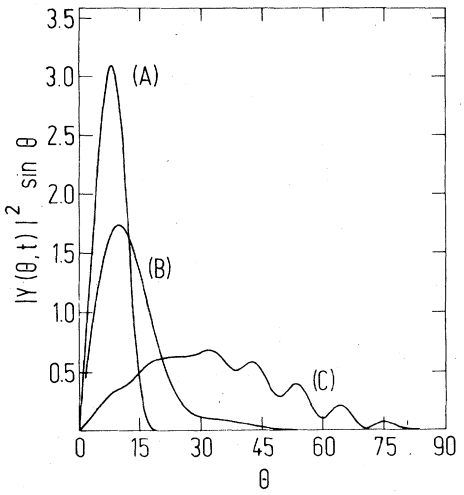

FIG. 4. The spreading of an angular wave packet in time for ^{238}U. The three curves correspond to the times, A ($t=0$), B ($t=0.32\tau_\beta$), C ($t=0.95\tau_\beta$).

tional motion in the energy region of interest in CF. No conclusion can be drawn from them, however, concerning the validity of semiclassical treatments[20] of Coulomb excitation induced by heavy ions. An essential ingredient of the semiclassical method, missing from the purely classical treatment, is the quantum mechanical interference of phases arising from different classical trajectories.

IV. PROMPT COULOMB FISSION

In this section we present some results which support the neglect of the direct couplings $V_{\mu E}$ of collective states to continuum states. This neglect is a practical necessity. Since the sudden approximation cannot be invoked to eliminate the rotational degrees of freedom and thus simplify the system, the coupled equations must be solved. The system solved in Ref. 8 consisted of 256 simultaneous, first-order differential equations. The solution of such a system involves a significant computational effort, even when using the RVM, which yields analytical formulas for many matrix elements. If the basis were expanded to include continuum states, the dimensions of the system would increase greatly, and the simplicity of the RVM would be lost. Such a calculation would be infeasible at present. Instead of attempting it, we here study a simple model of CF in order to get a rough estimate of the relative importance of the fast component.

Equation (3.1) forms the basis of this study. Only collisions with zero impact parameter are considered. We wish to reduce Eq. (3.1) to a one-dimensional system, which can be readily solved. Instead of using the sudden approximation, we assume that the rotational behavior of the system is essentially that of a rigid rotor, i.e., we write

$$\psi(\beta,\theta,t)\cong u(\beta,t)Y(\theta,t)\,. \tag{4.1}$$

The function $Y(\theta,t)$ is known; it is the solution of Eq. (3.2). It describes a time dependent orientation of the system. The function $u(\beta,t)$ is to be determined; it describes the breakup of the system. The exact solution of Eq. (3.1) can be written

$$\psi(\beta,\theta,t)=\sum_I u_I(\beta,t)Y_{I0}(\theta,0)\,. \tag{4.2}$$

Substitution of Eq. (4.2) into Eq. (3.1) results in a set of coupled partial differential equations. One can see the relation of the function u to the u_I by expanding $Y(\theta,t)$ in spherical harmonics,

$$Y(\theta,t)=\sum_I a_I(t)e^{-i\epsilon_I t/\hbar}Y_{I0}(\theta,0)\,. \tag{4.3}$$

The assumption, Eq. (4.1), is equivalent to

$$u_I(\beta,t)\simeq a_I(t)e^{-i\epsilon_I t/\hbar}u(\beta,t)\,.$$

Thus, the function u represents the average behavior of the functions u_I. Substitution of Eqs. (4.1) and (4.3) into Eq. (3.1) results in the one-dimensional Schrödinger equation obeyed by u:

$$\begin{aligned} i\hbar\frac{\partial u}{\partial t}&=\Big\{H_v(\beta)+\sum_I|a_I(t)|^2\frac{I(I+1)}{\hbar^2}\Big[\frac{1}{\Theta(\beta)}-\frac{1}{\Theta(\beta_0)}\Big]\\ &\quad+\overline{V}(\beta,t)\Big\}u(\beta,t)\,,\\ \overline{V}(\beta,t)&=\sum_I\sum_{I'}a_I(t)^*a_{I'}(t)e^{i(\omega_I-\omega_{I'})t}\\ &\quad\times\langle Y_{I0}|\,V(\beta,\theta,t)\,|Y_{I'0}\rangle\,. \end{aligned} \tag{4.4}$$

The quantity $\overline{V}$ is the perturbing monopole-quadrupole interaction, averaged over orientations. The second term in the effective Hamiltonian is the rotation-vibration coupling; $\Theta(\beta)$ is the moment of inertia.

The physics of prompt fission and its relationship to the coupled equations is illustrated schematically in Fig. 5. The potential energy U in H_v is sketched. The broken line in Fig. 5(a) represents U_0, the RVM potential. The arrows indicate Coulomb excitation followed by fission. The wavy arrow represents the neglected direct couplings to the continuum. In Fig. 5(b) a different but equivalent viewpoint is illustrated. The total potential energy function is sketched for two limiting cases, $\theta=0°$ and $\theta=90°$, for U on U at a separation distance of 21 fm. For $\theta=90°$, the top of the effective barrier drops below the energy of the unperturbed ground state. (At distances smaller than 20 fm, Coulomb-nuclear interference begins to raise the

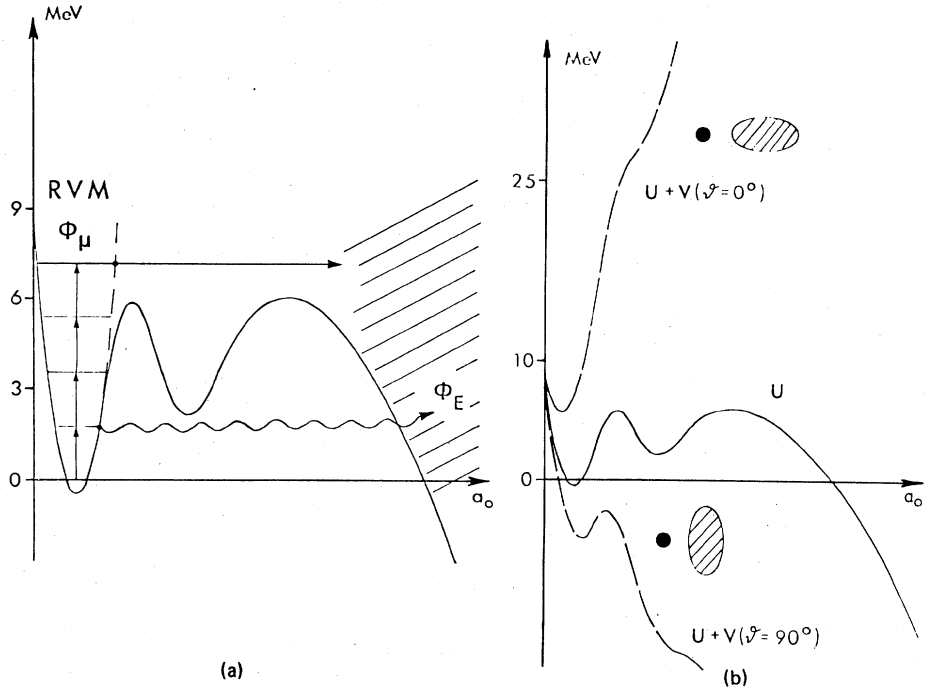

FIG. 5. (a) Schematic illustration of the OHG model of Coulomb fission, showing Coulomb excitation (vertical arrows) and the neglected process (wavy arrow) of direct excitation of continuum states. (b) Raising and lowering of the fission barrier due to the monopole-quadrupole interaction for $U-U$ at 21 fm separation. The insets show the angles (0° and 90°) between the nuclear symmetry axis and the separation coordinate r.

barrier.) One can think of prompt fission as fragments escaping while the barrier is low. Prompt fission events clearly should be emitted at angles of about 90°. The dynamical orientation shown in Fig. 3 is favorable to prompt fission. This orientation is built into our model by virtue of Eq. (4.1).

In order to solve Eq. (4.4) we must develop a physically reasonable model for the barrier U, the collective mass parameter $B(\beta)$, the moment of inertia $\Theta(\beta)$, and the interaction $V(\beta,\theta,t)$. A connection must be made between the collective variable β and the fragment separation coordinate for large values of β. The parameters B and Θ should be consistent with the known properties of low energy collective excitations in heavy nuclei for $\beta\sim\beta_0$. For large β they should agree with the reduced mass and moment of inertia of separated fragments. These matters are discussed in some detail in the Appendix.

Using the parameters described in the Appendix, Eq. (4.4) was solved with an initial wave function $u_0(\beta,t)$, consisting of the ground state of the harmonic oscillator potential U_0. A number of different cases were studied, for a variety of projectiles and Actinide targets, at energies of 80% of the Coulomb barrier. The parameters in $B(\beta)$ and $\Theta(\beta)$ were varied to determine the sensitivity of our results to these parameters. All cases studied followed the same pattern, illustrated in Figs. 6(a) and 6(b) for the case ^{238}U on ^{238}U. The mass parameter set A defined in the Appendix was used. The value of the moment of inertia, Θ_1, at the location of the second minimum was set equal to $150\hbar^2/\mathrm{MeV}$.[21] In Fig. 6(a) the gross behavior of the wave function is shown as a function of time. The quantity plotted is

$$\rho(x,t) = |u(x,t)|^2[B(x)]^{1/2}. \tag{4.5}$$

The coordinate x is a dimensionless fission coordinate, related to β. In the Appendix, x is defined and the normalization of Eq. (4.5) explained. Figure 6(a) is a small-scale plot of $\rho(x,t)$ in the vicinity of the first minimum. The dashed line is the effective potential in Eq. (4.4), consisting of U, $\bar{V}$, and the rotation-vibration coupling. The curves are labeled by the distance of projectile and target as in Fig. 3. On this scale there is no evidence for fission, i.e., loss of probability from the nuclear interior. The collision causes the packet to oscillate in the potential well. This can be thought of as the excitation of beta vibrations. In Fig. 6(b), the tail of ρ is plotted on an expanded scale for x values in the neighborhood of the second minimum of U and the saddle point. For separations of 85 fm on the outgoing branch of the Rutherford trajectory, ρ is negligible at the sad-

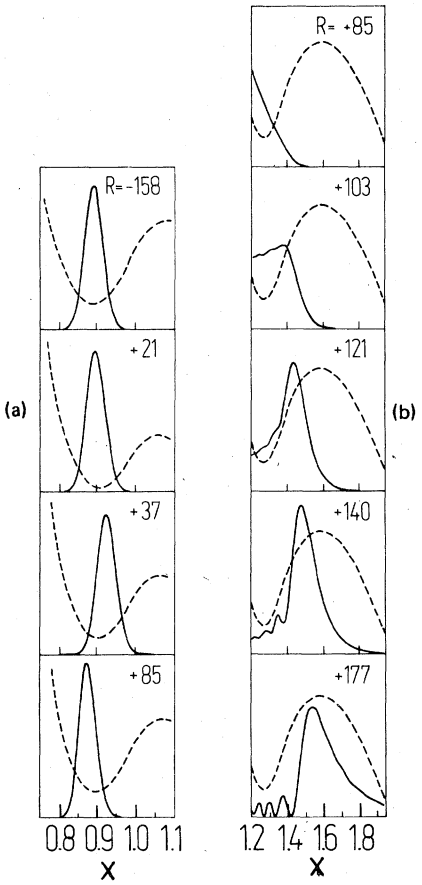

FIG. 6. (a) Plot showing the behavior of the probability density $\rho(x)$ as a function of time. The numbers in each figure give the separation, in fm, of the ions on the Rutherford trajectory. (b) Magnified picture of $\rho(x)$ in the vicinity of the second minimum and saddle points of the potential energy surface, showing fission taking place.

dle point. At later times there is a slow buildup of a small "bump" which eventually escapes through the barrier. At times corresponding to separations of 150 fm, there is a rapid buildup of ρ in the vicinity of the saddle point. The fission probability $P(t)$ can be obtained by integrating ρ in the exterior region or from the time integral of the probability flux, evaluated at the saddle point. This quantity is plotted in Fig. 7 for a number of different projectiles and targets. The calculations are all based on choice A of Fig. 11 of the inertia function and $\Theta_1 = 150\hbar^2/\mathrm{MeV}$. The two ^{132}Xe on ^{238}U cases are at energies of 70% (2) and 85% (1) of the Coulomb barrier. All other cases correspond to 80% of the Coulomb barrier. The curves all show a very small prompt component followed by a sharp rise at separation distances of order 135 fm. The fission probabilities at later times depend sensitively on the bombarding energy

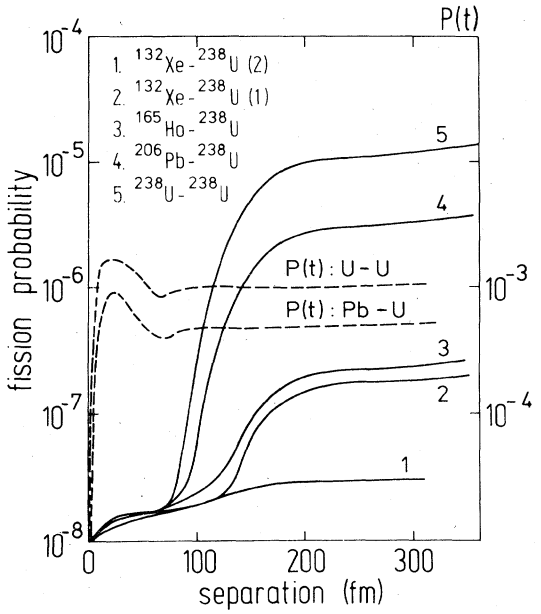

FIG. 7. Plot of fission probabilities as a function of time (solid curves). The calculations are based on choice A of Fig. 11 and $\Theta_1 = 150\hbar^2/\mathrm{MeV}$. The two Xe-U cases are at energies $0.7E_c(2)$ and $0.85E_c(1)$. All other cases are for $0.8E_c$. The dashed curves show the quantity $p(t)$ defined in Eq. (4.6); the results are taken from Ref. 7.

and projectile charge. This is completely consistent with the predictions of *asymptotic CF*. The prompt component is extremely small and insensitive to changes in these variables. Further results reported in the Appendix indicate that the qualitative features of Figs. 6(a), 6(b), and 7 are relatively insensitive to the parameters chosen. It is possible to compare these results to those of asymptotic CF. The function $P(t)$ is analogous to the quantity

$$p(t) = \sum_{\mu} |a_{\mu}(t)|^2 , \tag{4.6}$$

in which the sum is over RVM levels lying above the barrier. The models employed for prompt and asymptotic CF are sufficiently different that one should not expect these quantities to agree in magnitude; however, a comparison of their time dependences is very enlightening. The dashed curves in Fig. 7 give the function $p(t)$, Eq. (4.6), for the cases ^{208}Pb-^{238}U and ^{238}U-^{238}U. Comparing the rapid rise in $p(t)$, the population of fissionable levels, with the long delay in $P(t)$, indicates that the two-step picture of CF is very probably correct. The nucleus is excited near the closest approach point, then decays much later.

We conclude that the prompt fission mechanism is unimportant. This is due to the short time of the collisions. The collision time is of order τ_{β} or

less, but this is the characteristic response time. Lowering the fission barrier is like opening a door. The fragments try to leave but move too slowly. Raising the barrier shuts the door, driving the wave function back toward the first minimum and adding vibrational energy to the system. The alignment about 90°, therefore, does *not* produce the most favorable condition for CF. The magnitude of the repulsive $\Theta = 0°$ interaction is much greater [see Fig. 5(b)] than the attractive $\Theta = 90°$ interaction. Since the mechanism of CF is pumping energy, rather than opening a door, collisions with $\Theta = 0°$ would be much more effective in producing CF, as originally suggested by Beyer and Winther.[3]

V. CALCULATION OF FISSION PROBABILITIES

In this section we describe a model for the spreading of the collective states φ_μ and for the decay widths in Eq. (14). Results of calculations based on this model will then be presented. In developing such a model, we have tried to keep it as simple as possible. Because CF is such a complex process, involving states with a wide range of energies (0–15 MeV) and angular momenta (0–30), the construction of more realistic models will be a formidable job and is probably not justified by the present state of our experimental knowledge. Because our experimental knowledge is so limited, the construction of more complicated models at this time would probably result in a proliferation of free parameters—more than can be fitted to available data. Although it is simple, we have tried to make this model consistent with existing data on neutron, gamma, fission, and spreading widths. We believe the results are reasonably accurate, and that the model indicates the important physical effects and direction for future work.

A. Spreading of the collective states

The spreading of the collective levels φ_μ into a background of compound states is but one example of a phenomenon frequently occurring in nuclear physics.[22] As a result of matrix elements $H_{\mu k}$, connecting the collective states to the noncollective states φ_k, there is a spreading width

$$\gamma_\mu = 2\pi D |H_{\mu k}|^2 . \tag{5.1}$$

The quantity D is the average spacing of energy levels ϵ_k and is the inverse of the level density $\rho(\epsilon_k)$. The strength of φ_μ is spread over an energy interval of order γ_μ. The energy dependence of $|A_\mu(E)|^2$, the probability of φ_μ in a compound state of energy E, is approximately of Breit-Wigner form,

$$|A_\mu(E)|^2 \approx \frac{S_\mu}{(E-\epsilon_\mu)^2 + \frac{1}{4}\gamma_\mu^2} . \tag{5.2}$$

In our calculations, we treat E as a continuous variable. The constant S_μ is fixed by the normalization condition

$$\rho(\epsilon_\mu) \int |A_\mu(E)|^2 dE = 1 . \tag{5.3}$$

The density is not included in the integrand. This is because the Lorentzian falls slowly with energy at large E, whereas ρ increases exponentially. The normalization integral in Eq. (5.3) would therefore diverge if the upper limit were taken to be infinity. In addition, the long tail of the Lorentzian gives other unphysical results which will be discussed later. They necessitate restricting the integration in Eq. (2.19) to a fairly narrow energy interval (~1 MeV) around ϵ_μ. This approach is, of course, oversimplified and does not properly account for the strongly damped states.

The quantity γ_μ is extremely difficult to determine. No reliable microscopic model is available for the matrix elements $H_{\mu k}$. One might assume a proportionality between γ_μ and ρ; however, because of the exponential rise in ρ with energy, this assumption results in increases of orders of magnitude in γ_μ over an energy increase of a few MeV. A more reasonable approach is that suggested by Lynn,[23] who pointed out that the relevant density in Eq. (5.1) is that of the states φ_k which couple directly to φ_μ. These "relevant" states can be described by the collective model. Consider the vibrational and intrinsic parts of a collective model wave function,

$$\varphi_n(\beta)\chi_g(\beta_0; x_1, \ldots, x_n) .$$

For simplicity only the beta vibrational and intrinsic ground state parts of the wave function are written down. The $\{x_i\}$ are a set of intrinsic space-spin coordinates. In the collective model these states interact with states

$$\varphi_{n-1}(\beta)\chi_e(\beta_0; x_1, \ldots, x_n) ,$$

in which χ_e is a one-particle, one-hole state built on the ground state χ_g. These states are coupled by the particle-surface coupling. This is obtained in the usual way, by expanding the single-particle potential, for arbitrary deformation β about the equilibrium shape β_0. The first order term results in a coupling matrix element,

$$\langle \varphi_n \chi_g | V_{ps} | \varphi_{n-1}\chi_e \rangle \propto (n+1)^{1/2} .$$

In this model, the density of relevant states χ_e does not vary with energy. The squared matrix element in Eq. (5.1), however, increases in proportion to $n+1$, or roughly in proportion to the ex-

citation energy. For ^{238}U there is evidence that in the first well near the barrier top $\gamma_\mu \approx 1$ MeV, and that in the second well $\gamma_\mu \approx 100$ keV. These results are reproduced roughly by

$$\gamma_\mu \text{ (MeV)} \approx 0.3E \text{ (MeV)} - 0.5 , \tag{5.4}$$

where E is measured from the bottom of the appropriate well. We use this relationship in our calculations. For $E \approx 1$ MeV, $n=1$, the formula predicts negative values, and γ_μ is set to zero, corresponding to zero spreading of the lowest beta vibration. For angular momenta, $I>0$, the energy E in Eq. (5.4) is measured from the yrast level of that spin.

Clearly, the above arguments are quite primitive. In reality, the $n=1$ vibrational state is a linear combination of low-lying particle-hole states. It lies below the pairing gap and does not spread. More highly excited vibrational states are located in a sea of more complex states and tend to dissolve into this background. Equation (5.4) is a simple ansatz which probably gives a reasonably accurate description of this spreading. No effort has been made to refine Eq. (5.4) by varying the constants.

A more correct theory of spreading would be based upon a "doorway state" approach.[24-27] In such theories, one couples all collective and compound states existing in both minima of the potential energy surface. However, there is simply not enough information available, experimental or theoretical, for us to develop a quantitative theory of this sort for the range of energies and angular momenta we must consider. Considering some of the other uncertainties in the theory, it would not be worth the effort.

B. Gamma ray widths

Two kinds of gamma ray processes compete with fission. The collective component φ_μ of the compound state can decay by $E2$ decay to a lower energy collective state. The noncollective components can decay to the lower lying odd-parity noncollective states by $E1$ emission. Decay to even-parity compound states by $M1$ emission is possible but is much weaker. The $E2$ widths are proportional to the probability $|A_\mu(E)|^2$. Similarly, we assume that the $E1$ emission rate is proportional to $1-|A_\mu(E)|^2$, the probability of noncollective states. Therefore, we write

$$\Gamma_\gamma = |A_\mu(E)|^2 \Gamma_\mu(E2) + [1-|A_\mu(E)|^2]\Gamma(E1) . \tag{5.5}$$

For the estimate of the $E2$ part, we assumed a single collective transition. For a level with $I>0$, this was calculated from the $B(E2)$ formula[17] for decay to the $I-2$ state of the same band. For $I=0$, we used the $B(E2)$ formula[17] for the transition, $0^+_\beta \rightarrow 2^+_{g.s.}$. For $E1$ decays we used the statistical model formula of Back *et al.*[18] for the total $E1$ width of a compound level decaying to all allowed compound states of lower energy,

$$\Gamma(E1;E;I) = KA^{2/3}\rho(E,I)^{-1} \sum_{j=|I-1|}^{I+1} \int_0^E \rho(\epsilon,j)(E-\epsilon)^3 d\epsilon . \tag{5.6}$$

The constant K is fitted to the known gamma width of a low energy neutron resonant state. Its value is 1.4×10^{-9} MeV^{-3}. The level densities for positive and negative parity are assumed to be equal.

C. Neutron widths

At energies above the neutron threshold, neutron emission becomes a very important competing process; therefore it is important to be able to make estimates of neutron widths which are reliable over a wide range of energies and angular momenta. We follow the approach of Britt *et al.*,[28] based on the continuum theory of nuclear reactions.[29] This formula is

$$\Gamma_n(E,I) = [2\pi\rho(E,I)]^{-1} \times \sum_j \sum_{s=|j-1/2|}^{j+1/2} \sum_{l=|I-S|}^{I+S} \int_0^{E-S_n} T_l(kR)\bar{\rho}(\epsilon,j)d\epsilon . \tag{5.7}$$

The neutron binding energy is S_n. The level densities in initial and daughter nuclei are denoted by ρ and $\bar{\rho}$, respectively. The T_l are transmission coefficients defined in the work of Blatt and Weisskopf.[29] The width computed from Eq. (5.7) is multiplied by $1-|A_\mu(E)|^2$ to get the width $\Gamma_n(E)$ for use in Eq. (2.19).

D. Fission widths

We write for the fission width in Eq. (2.19),

$$\Gamma_f = |A_\mu(E)|^2 \Gamma^f_\mu + [1-|A_\mu(E)|^2]\Gamma^f_c . \tag{5.8}$$

The width Γ^f_μ is the escape width of the collective state φ_μ. This is not the total fission width. At higher energies other transitional states become available to the compound system, resulting in the second width Γ^f_c, which can become quite large.

The fission width Γ^f_μ is given by

$$\Gamma^f_\mu(E) = \frac{\hbar\omega\beta}{2\pi} T_\mu(E) . \tag{5.9}$$

The quantity T is a penetrability, and $\omega_\beta/2\pi$ gives the number of assaults on the barrier per second. The penetrability T is computed as follows: Following Oberacker *et al.*[8] we define an effective barrier for a state of angular momentum I:

$$U_I(\beta) = U_\beta + \frac{\hbar^2 I(I+1)}{2\Theta(\beta)}. \tag{5.10}$$

The moment of inertia is chosen to be a linear function of the collective coordinate β as suggested by the data.[30,31] The function Eq. (5.10) can be rather well approximated by smoothly joined parabolas. For each I, such a fit was made and the penetrabilities of the resulting well were computed by the methods of Cramer and Nix.[32] The functions $T_\mu(E)$ show penetration resonances corresponding to states in the second minimum of the potential well. The computer program was written so that these could be suppressed; i.e., $T_\mu(E)$ could be replaced by a smooth monotonic curve following the nonresonant behavior. By making calculations with and without transmission resonances, the effect on CF of states in the second well could be roughly estimated.

The term Γ_c^f is the average fission width of a compound state proceeding through collective states other than φ_μ. These collective states are built on excited intrinsic states; φ_μ is built on the lowest intrinsic state χ_0. For energies near the barrier top and below, Γ_c^f is completely negligible, since the barriers for these other transitional states are higher than the barrier $U(\beta)$. The barrier $U(\beta)$ assumes adiabatic motion based on the lowest intrinsic state. At energies greater than the barrier height by the pairing gap Δ, these other transitional states become important. We follow the simple treatment of Vandenbosch and Huizenga.[33] For energies greater than $B_I + \Delta$, where B_I is the barrier height of the function U_I in Eq. (5.10), we assume penetrabilities of unity. For lower energies the penetrabilities are taken to be zero. The continuum theory is assumed. The result is

$$\Gamma_c^f = K'[2\pi\rho(E,I)]^{-1} \int_\Delta^{E-B_I} \tilde{\rho}(E',I)dE'. \tag{5.11}$$

The density $\tilde{\rho}$ is the density of states at the saddle point. The constant K' is an adjustable constant introduced to make it possible to normalize the theory to known values of the ratio Γ^n/Γ_c^f, measured in other reactions. The experimental data[33] seem to imply that this ratio has a value of about 5 and is approximately energy independent in the energy range 2–5 MeV above the neutron threshold. We adjusted the value of K' and also the parameters of $\tilde{\rho}$ so that these trends were reproduced by our equations for low values of the angular momentum. The value of K' is 0.2; the $\tilde{\rho}$ parameters are discussed in the next section. Results for the calculated ratio Γ^n/Γ_c^f are shown in Fig. 8 for several values of the angular momentum.

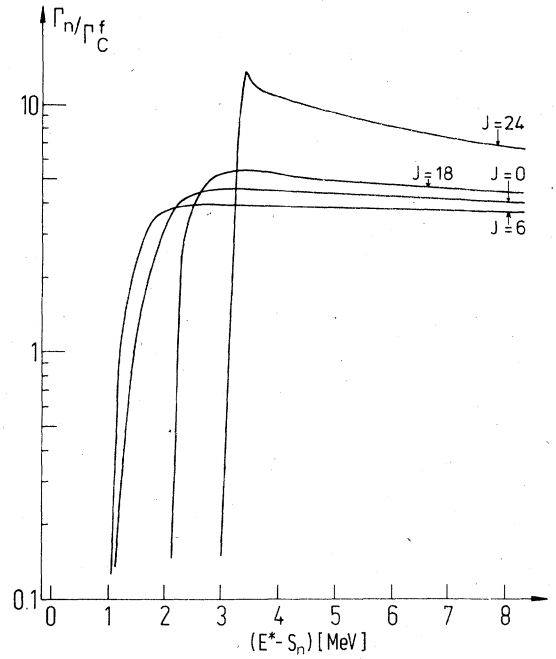

FIG. 8. Plots of the ratios Γ_n/Γ_c^f for compound states as functions of energy and angular momentum. The energy is measured above the neutron threshold.

E. Level density formula

The nuclear level density is used in Eqs. (5.6), (5.7), and (5.11). We need a level-density formula which is reasonably accurate over a large range of angular momenta, although extreme accuracy is not important, since our goal is not a precise theory of fission probabilities but only reasonable estimates. The density used in our calculations is[34]

$$\rho(E,I) = \frac{\sqrt{a}}{24}\left(\frac{\hbar^2}{2\Theta}\right)^{3/2} \frac{(2I+1)\exp\{2[aE_{\rm eff}(I)]^{1/2}\}}{[E_{\rm eff}(I)]^2}. \tag{5.12}$$

The effective energy $E_{\rm eff}$ is given by

$$E_{\rm eff}(E,I) = E - \Delta - E_{\rm yrast}(I). \tag{5.13}$$

We follow Gilbert and Cameron[35] and let $\Delta = 1.4$ MeV and $a = 28.5$ MeV^{-1} in ^{238}U. For the moment of inertia Θ, we use $\Theta = 102\hbar^2$ MeV^{-1}, which results in $\rho = 4.26 \times 10^4$ MeV^{-1} at the neutron threshold. (For comparison, the RVM and rigid rotor values of Θ are 67 and 131, respectively.) The yrast energies were taken from Oberacker's[8] RVM calculations. For odd spins, needed in the calculation of $E1$ widths, a linear extrapolation between even spins was made. The density $\tilde{\rho}$ was obtained from ρ with the following changes in parameters: $\tilde{\Delta} = 1.0$ MeV, $\tilde{a} = 1.05a = 29.9$ MeV^{-1}. We attribute no physical significance to these changes. We re-

gard Eq. (5.11) as merely a reasonable parametrization of Γ_c^f, with parameters chosen such that the Γ_n/Γ_f experimental data can be approximately reproduced. In order to calculate Γ_n, Eq. (5.7), we need density parameters for ^{237}U. In place of Eq. (5.13) we use

$$E_{\text{eff}} = E - \Delta' - \frac{\hbar^2}{2\Theta} I(I+1) . \tag{5.14}$$

The rigid-body value is used for Θ, $\Theta_r = \hbar^2 A^{5/3}/70$. The other parameters are $\Delta' = 0.7$ and $a = 27.8$ MeV^{-1}.

F. Results for the fission probability

We calculated the fission probability using Eq. (2.19) and widths computed as outlined above. In Fig. 9 the excitation function for $^{184}_{74}\text{W} + ^{238}_{92}\text{U}$ at $\theta_{\text{c.m.}} = 180°$ is shown. The results of the sharp cutoff model shown in Fig. 9 are lower than those shown in Fig. 1 by a factor of 1.1 to 1.6, depending on the energy. This is because of an error in the earlier calculations arising from an incorrect RVM matrix element, $\langle I, K'=2, n_2'=0, n_0'=0 | H | I, K=0, n_2=2, n_0=0 \rangle$, in Ref. 36. One sees that the sharp cutoff model and the full calculation (including barrier penetration, damping, and γ/n competition) bracket the data in the sub-Coulomb region. The improved treatment results in CF cross sections greater by a factor of about 3. The results turned out to be somewhat sensitive to the functional form of $|A_\mu(E)|^2$, Eq. (5.2). Our earliest calculations yielded a fission probability approximately 5 times greater than the sharp cutoff results of Oberacker *et al.*[8] This large increase in fission probability was the result of the term Γ_c^f, which increases rapidly with energy. The Lorentzian has such a long tail that, associated with each collective state ϕ_μ, there results a large contribution to fission from compound states several MeV higher in energy. This is unphysical and can be remedied by the choice of a function, such as a Gaussian, which falls more rapidly to zero with $|E - \epsilon_\mu|$. We chose simply to restrict the integration limits, so that no two levels of the same spin had any overlap. For levels with a large spreading width γ_μ, this is equivalent to assuming uniform spreading on a finite interval. This greatly reduced the fission probabilities.

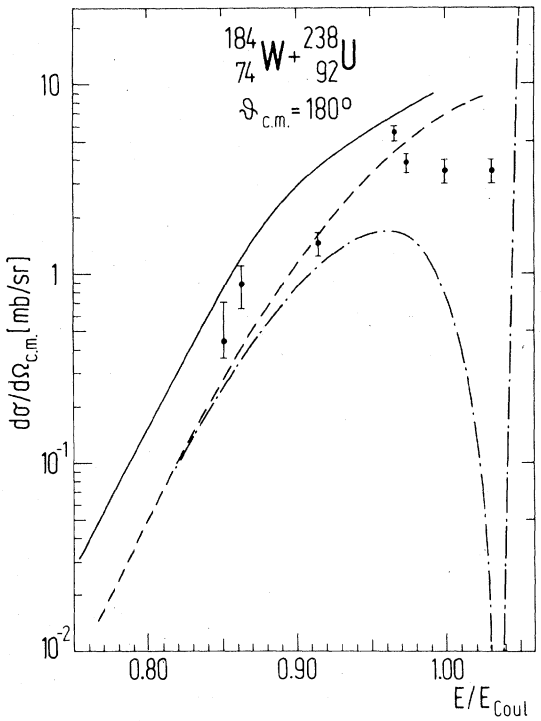

FIG. 9. Theoretical cross sections for Coulomb fission and fission following inelastic nuclear excitation in comparison with the experimental data (Ref. 9). Solid curve: pure CF cross section including barrier penetration, damping into noncollective levels and γ/n competition [see Eq. (2.19]. Dashed curve: pure Coulomb fission in the simplified sharp cutoff model (Refs. 8 and 14). Dot-dashed curve: fission following Coulomb and inelastic nuclear excitation (real Yukawa potential) in the sharp cutoff model.

In order to understand the origins of the difference between the sharp cutoff and the extended calculations, let us examine in detail the case $E/E_c = 0.85$. The sharp cutoff model yields a fission probability of 1.1×10^{-3}. The calculations of the present model yield 3.0×10^{-3} when transmission resonances are suppressed and 3.6×10^{-3} when they are included. Since it is well known that there is damping in the second well, comparison of the results with and without transmission resonances somewhat overestimates their importance. We conclude that they contribute, at most, about 15% to the CF cross section. The full curve in Fig. 9 is calculated *with* the transmission resonances.

For states near the barrier top, the fission probability lost by gamma-ray competition is more than compensated for by that gained by the barrier penetration of states below the barrier top. At higher energies, neutron emission becomes very important, but its effect is partially compensated for by the availability of new transition states for fission. Although Eq. (2.19) is a sum over many small numbers, we can see what is happening by inspection of the histogram in Fig. 10. In this histogram the total contribution of all states of a given angular momentum is plotted against angular momentum. The sharp cutoff results are compared to the results of the more realistic model. In the latter case, the effect of states below the barrier top is indicated, show-

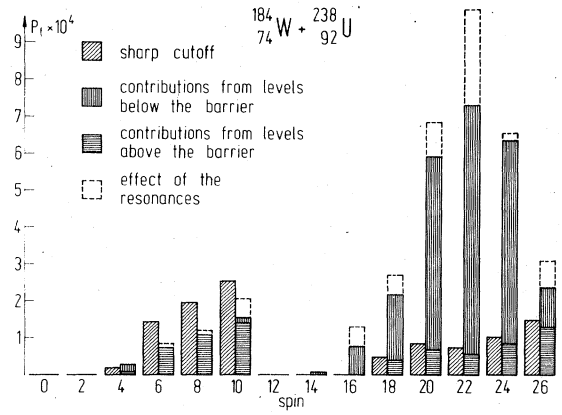

FIG. 10. Histogram indicating the differences between the predictions of fission probabilities of the sharp cutoff model and the extended model. The contributions of levels below the barrier, above the barrier, the contribution of penetration resonances in the second minimum of the double-humped well are indicated. The bombarding energy is $E = 0.85E_c$.

ing the importance of barrier penetration. One sees that, in each case, the contribution of states above the barrier is decreased slightly due to damping. The states of high angular momentum are most strongly enhanced by barrier penetration effects. This is because there are strongly excited, high angular momentum states just below the barrier which are left out of the sharp cutoff calculations. Because their populations $|a_\mu|^2$ are large, they make a large contribution by barrier penetration. The amplitudes of the low-spin states just below the barrier top are significantly smaller, because more steps of Coulomb excitation are required to reach these states.

Quantitatively, these effects are somewhat energy dependent. The new fission probabilities are increased by factors of 3.9, 3.3, and 2.0 at $E/E_{\mathrm{Coul}} = 0.77$, 0.85, and 0.935, respectively, compared to the sharp cutoff model. This can be easily understood; with increasing bombarding energy, the mean excitation energy rises, and hence the penetration effects from levels below the fission barrier become less important. For incident energies above the Coulomb barrier, one would expect both curves to become almost equal.

VI. SUMMARY AND CONCLUSIONS

In this paper we have studied a number of different aspects of Coulomb fission dynamics. Our motivation has been to examine the validity of the Oberacker-Holm-Greiner model and improve on it. The results of the paper can best be understood and summarized by relating them to the following questions concerning the OHG model:

(1) Does Coulomb fission indeed proceed in two steps, Coulomb excitation followed by spontaneous fission?

(2) Can the Coulomb excitation step be calculated accurately by treating all collective states as if they were bound?

(3) Can the fission probabilities in the second step be calculated accurately from a simple, sharp-cutoff model?

A theoretical framework is presented which is a unified treatment of Coulomb excitation, fission, and competing processes. The collective states are treated in a formally exact way as bound states imbedded in a fission fragment continuum. The formalism allows for the spreading of these collective states into noncollective compound states. By including other continua, the competing processes (gamma-ray decay and neutron decay) are taken into account.

In terms of this framework, questions (1) and (2) are shown to be closely related. If the quasibound collective states correspond to sharp resonances, then treating them as bound states and neglecting direct couplings to the continuum is a good approximation. Sufficiently sharp resonances correspond to narrow escape widths and thus long lifetimes relative to the collision time, in agreement with the two-step mechanism. The Coulomb excitation of broad resonances cannot be treated accurately in terms of the quasibound states, and they may decay appreciably during the collision. Put in another way, if the resonances are broad, one cannot neglect direct couplings to the fission fragment continuum, and these couplings result in prompt rather than asymptotic Coulomb fission. Since the widths of the highly excited collective states are not reliably known, we cannot resolve these questions in a definite way. However, the exact integration of the Coulomb fission problem in one dimension (Sec. IV) yields a time dependence which strongly supports the asymptotic CF mechanism.

We approached question (3) by attempting to make a more realistic model for the fission probability which includes the spreading or "damping" of the collective states into the background of noncollective compound states and the competing decay channels. In the case of small or moderate spreading, we showed that the amplitudes a_μ computed without spreading can be used in a simple formula for the fission probability which includes spreading and competing processes. No simple modification of the theory of Oberacker *et al.*[8] has been devised which is correct in the case of large spreading.

Numerical model calculations of fission probabilities are discussed in Sec. V. These indicate that the sharp cutoff model underestimates fission

probabilities by a factor of 2 or 3. The increase in fission probability is essentially a barrier penetration effect; the effect is more pronounced for low incident energies than for higher ones. We also see from Fig. 10 that high-spin contributions, i.e., spin 18 to 26, are significantly enhanced compared to contributions from lower spins. The enhancement of CF for states below the barrier by coupling to states in the second minimum of the well is small but significant.

One should keep in mind that the absolute cross sections computed by either the sharp cutoff model or the improved model are sensitive to the barrier parameters used. We could have improved the agreement of both models with experiment by changing the barrier parameters of Ref. 18 within their error bars; however, we did not. An agreement within a factor 2 or 3 supports the sharp cutoff model as a first approximation. However, we strongly suggest the use of the improved model, especially for predictions concerning the details of CF, such as angular distributions, dependence on projectile charge and others.

On the other hand, the new version of the theory results in CF cross sections greater than those of Backe *et al.*[9] by a factor of about 2, depending on energy, which suggests that physical effects have been neglected which are of the same importance as those already included in the extended model. It is easy to identify a number of reasons why the calculations overestimate the CF cross section. One obvious reason is the neglect of nuclear forces in the present calculations; we decided to study their influence separately since the Coulomb-nuclear interference problem is not yet completely understood. Another reason is the use of the RVM. Although the RVM gives a rather good account of the energies and electromagnetic properties of the ground state and gamma bands, it overestimates the $B(E2)$ value for $0_g^+ \rightarrow 2_\beta^+$. Therefore, the $|a_\mu|^2$ of highly excited states, computed in Ref. 8, are probably too large. On the other hand, the octupole states of ^{238}U are highly excited in heavy-ion Coulomb excitation experiments. These bands have been left out in all calculations to date. Correcting the RVM for overpredicting the excitation of beta vibrations and including octupole bands should be the direction of the theory in the immediate future. All of these improvements can be included in a straightforward way in the present approach.

We have also investigated the possibility of simplifying the treatment of the rotational motion by using the sudden approximation. The results reported in Sec. III show that this approximation is not valid for Coulomb fission. The full coupled equations treatment is necessary.

Over the years great strides have been made in understanding fission. The theoretical developments have tended to follow experimental developments. Coulomb fission will probably be no exception. At present there is an excessive richness of theoretical speculation; however, as more data become available, we are confident that CF will be a valuable source of information on the importance of various multipoles, the potential energy surface, moments of inertia and collective mass parameters for large deformations.

APPENDIX: THE PROMPT FISSION MODEL

In this appendix the prompt fission model is discussed. A reader requiring more details can find them in Refs. 7 and 37. Since this model was not developed in order to make reliable predictions about fission yields, but only to give an idea of how fission events develop in time, it is accordingly very simple and phenomenological, but with as much realism as possible incorporated.

The fission coordinate X

For deformations between equilibrium and scission we assume an axially symmetric nuclear surface, described by

$$R(\theta') = CR_0[1 + bP_2(\cos\theta')]. \tag{A1}$$

The symmetry axis is the Z' axis and θ' is the polar angle. The spherical shape is defined by $C = 1$, $b = 0$. For $b \neq 0$ the value for c is found by requiring volume conservation. We define a length xR_0 to be the distance between the mass centers of equal halves, resulting from dividing the nucleus by a plane perpendicular to the symmetric axis. For a spherical shape, $x = \frac{3}{4}$. Beyond scission, xR_0 is defined to be the separation of the fission fragments. The value of x can be related to b and c using Eq. (A1). The nuclear shapes described by the parameter b in the immediate vicinity of the scission point are not completely adequate. In spite of this we feel that the coordinate x will describe the dynamics of fission reasonably.

The vibrational inertia B

We write the vibrational kinetic energy in terms of a variable mass parameter $B(x)$

$$T_v = -\frac{\hbar^2}{2}\frac{1}{[B(x)]^{1/2}}\frac{\partial}{\partial x}\frac{1}{[B(x)]^{1/2}}\frac{\partial}{\partial x}. \tag{A2}$$

This has the consequence[17] that the solutions to Eq. (4.4) must be normalized according to

$$\int_{-\infty}^{+\infty} |u(x,t)|^2 [B(x)]^{1/2} dx = 1. \tag{A3}$$

We choose a simple formula for B which contains parameters which can be adjusted so that B has correct properties in two limits, viz., near the equilibrium deformation x_0 and for separated fragments, i.e.,

$$T_v \sim -\frac{\hbar^2}{2\mu R_0^2}\frac{\partial^2}{\partial x^2}, \quad x \to \infty. \tag{A4}$$

In Eq. (A4) μ is the reduced mass of the fission fragments. Between the two limits, the shape of the function $B(x)$ should also be adjustable, so that we can determine how sensitive our results are to the shape of the function, B. A convenient form for $B(x)$ is

$$B(x) = A\left\{1 + B_1 \exp\left[\frac{x_0 - x}{C_1}\right] - B_2 \exp\left[\frac{x_0 - x}{C_2}\right]\right\}^2, \tag{A5}$$

$$A = \mu R_0^2.$$

The parameters of the first exponential are adjusted to determine the overall shape; the parameters of the second are adjusted so that $B(x)$ is slowly varying near $x = x_0$. The inertia is given a square to facilitate the use of $B(x)$ in expressions such as Eq. (A3). In Fig. 11, B is plotted for several parameter sets which were used in the calculations. The parameter values corresponding to each curve are also shown on the figure.

The fission barrier U

We represent the fission barrier as smoothly joined parabolas. The barrier parameters of

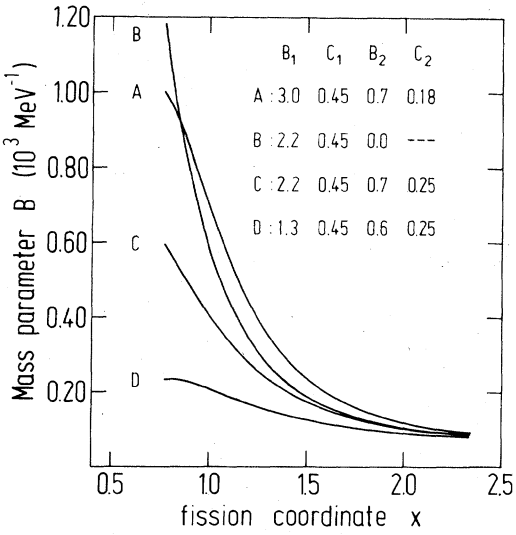

FIG. 11. Mass parameters $B(x)$ are shown for ^{238}U for different values of the parameters B_1, C_1, B_2, and C_2.

Back *et al.*[18] were used. These parameters result from the analysis of transfer fission data involving light ions. The data analysis depends on barrier penetrabilities, which in turn depend on the barrier parameters. For smoothly joined parabolas and for an inertia B which is constant, i.e., not a function of deformation, the penetrabilities are mass independent.[32] In the present study B is taken to be a function of x. In order to use the experimentally determined barrier parameters consistently with a deformation dependent mass, we make the following change of variable. A new coordinate y is introduced, defined by

$$y = \int [B(x)]^{1/2}\, dx. \tag{A6}$$

Because of the simple form, Eq. (A5) chosen for B, Eq. (A6) is easily integrated, yielding an analytical form for $y(x)$. In terms of y, the vibrational Hamiltonian can be written

$$H_v = -\frac{\hbar^2}{2}\frac{\partial^2}{\partial y^2} + \tilde{U}(y). \tag{A7}$$

The barrier $\tilde{U}$ is constructed from smoothly joined parabolas in the variable y, using the parameters of Ref. 18. This means that the penetrabilities of our H_v are consistent with the transfer data. Given $U(y)$ and $y(x)$, the barrier $U(x)$ can be constructed for any choice of B_1, B_2, C_1, and C_2 in Eq. (A5). We find it more convenient to work with x; however, one could equally well transform all the quantities in Eq. (4.4) into functions of y.

The location x_0 of the first minimum of U is determined by the intrinsic quadrupole moment of the ground state band. At large x, U should join smoothly to the Coulomb repulsion of the fission fragments, i.e.,

$$U(x) \sim \frac{Ze^2}{4xR_0} - T_f, \quad \text{large } x. \tag{A8}$$

The quantity T_f is the total kinetic energy acquired by the fragments. In fitting the parabolic part of U to Eq. (A8), we treated T_f as an adjustable parameter; however, its values always stayed in a reasonable range, between 150 and 200 MeV. The parabolic barrier and the asymptotic form Eq. (A8), are joined by a cubic splice. The resulting U functions, and their dependence on the mass function B are shown in Fig. 12.

Moment of inertia Θ

The moment of inertia function $\theta(x)$ should vanish at the spherical shape $x = 0.75$. For $x = x_0$, the value of $\theta(x_0)$ can be determined from the $2_g^+ - 0_g^+$ energy spacing. For large x, it should approach

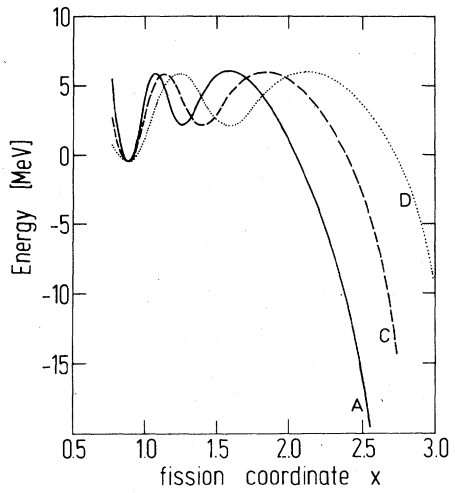

FIG. 12. Fission barriers $U(x)$ used in the present study, corresponding to different mass parameters. The curves are labeled according to the parameter sets of Fig. 11.

$$\theta \sim Ax^2 = \mu R_0^2 x^2, \quad \text{large } x. \tag{A9}$$

Between $x = x_0$ and $x = x_1$, the location of the second minimum, there is evidence[30,31] that θ varies linearly with deformation. To achieve these properties the range of x values is divided into 4 regions, and $\theta(x)$ is represented by a different polynomial in each region. The polynomials are joined smoothly at the boundaries. The function $\theta(x)$ used for ^{238}U is shown in Fig. 13. The value $\theta(x_1) = 150\hbar^2/\text{MeV}$ was used in most calculations; however, calculations were also performed with the value $200\hbar^2/\text{MeV}$.

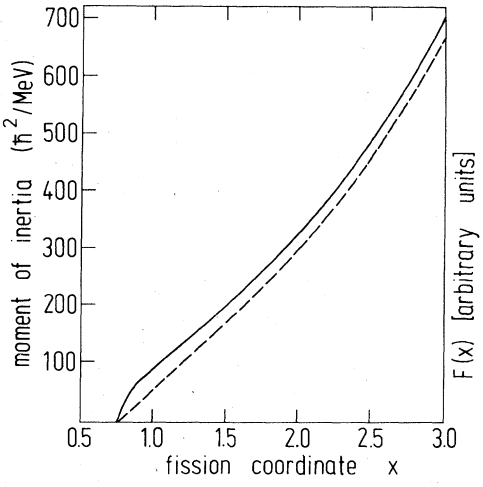

FIG. 13. Solid curve: The moment of inertia Θ for ^{238}U as a function of the fission coordinate X. Dashed curve: The function $F(x)$ of the monopole quadrupole interaction as a function of the fission coordinate x.

The monopole-quadrupole interaction V

The interaction V is given by

$$V = \frac{Z_1 e^2}{r(t)^3} \int \rho(\vec{r}\,')r'^2 P_2(\cos\omega) d^3r', \quad r(t) > r', \tag{A10}$$

where $\vec{r}\,'$ is an intrinsic coordinate of the nucleus and ω is the angle between $\vec{r}$ and $\vec{r}\,'$. For a uniform density within the surface defined by Eq. (A1), the integral in Eq. (A10) can be computed analytically. For values of x beyond scission, the target is thought to consist of two equal point charges separated by a distance xR_0. In both cases V is of the form,

$$V = \frac{F(x)}{r(t)^3} P_2(\cos\theta). \tag{A11}$$

The function $F(x)$ resulting from Eq. (A10) and the asymptotic form are smoothly joined by a cubic spline. The resulting function is shown in Fig. 13.

The form Eq. (A10) for V is valid only for $r(t) \geq R_0 x/2$. For $^{238}\text{U} - ^{238}\text{U}$ collisions, the smallest value of r is about 21 fm; R_0 is about 7 fm. The validity criterion is thus $x \leq 6$. Calculations show that $u(x,t)$ remains localized well inside this distance during the collision time.

Calculations

For the solution of Eq. (4.4) and the other differential equations, a computer program was developed based on the standard Crank-Nicholson algorithm.[38] This method is very stable against the propagation of round-off errors. Calculations were carried out on a DEC-10 computer. On this computer, each case studied required about one hour of CPU time. The initial state was chosen to be a ground state harmonic oscillator wave function, in the coordinate y. With this initial wave function and V set to zero, it was found that $|u|$ changed negligibly over time intervals very large compared to a collision time.

When the interaction is not zero, the initial state is perturbed by the time dependent effective interaction $\bar{V}(x,t)$ defined by Eq. (4.4). In Fig. 14 is plotted the expectation value of $\bar{V}$, i.e.,

$$\langle \bar{V} \rangle = \int dx [B(x)]^{1/2} |u(x,t)|^2 \bar{V}(x,t). \tag{A12}$$

The case illustrated is $^{238}\text{U} - ^{238}\text{U}$ at 80% of the Coulomb energy. The abscissa is the separation coordinate r, on the outgoing branch of the Rutherford trajectory. The maximum effective interaction occurs a short distance beyond the closest approach distance of 21 fm. This occurs because of the alignment, shown in Fig. 3, which reaches

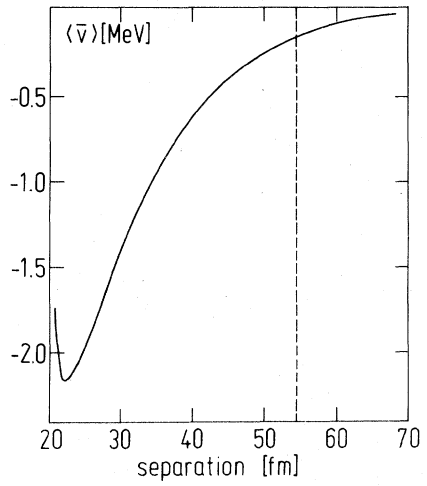

FIG. 14. The expectation value $\langle\bar{V}\rangle$, Eq. (A12), as a function of ion separation on the outgoing branch of the Rutherford trajectory.

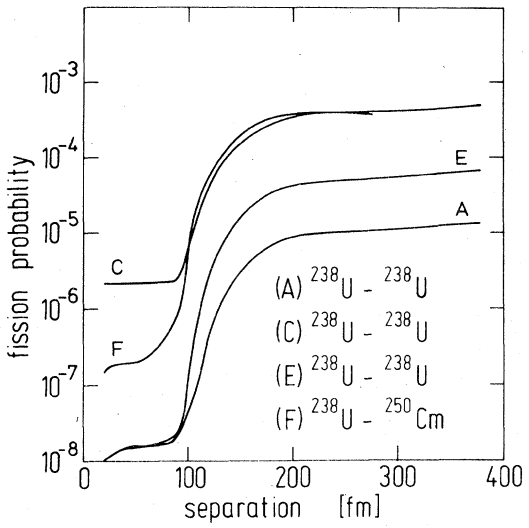

FIG. 15. Plot of fission probabilities as a function of time to test the sensitivity of prompt Coulomb fission to the parameters of the model (A, C, E) and the fissibility of the target (F). Incident energy: $E = 0.8E_c$.

its maximum after closest approach. The dashed line in Fig. 14 indicates the distance corresponding to a time of 0.5 τ_β after closest approach. From Fig. 14 it is clear that the perturbation $\bar{V}$ is "turned on" for a time short compared to a beta vibration. The fission probability $P(t)$ was obtained from the time-integrated flux at the saddle point, using the quantum-mechanical flux appropriate to Eq. (4.4).

The results of calculations have already been illustrated in Figs. 6, 7, and 8. In Fig. 15, some additional results are plotted for the collision systems ^{238}U – ^{238}U and ^{238}U – ^{250}Cm. The case labeled (A) is the same ^{238}U – ^{238}U case in Fig. 8. Case (C) corresponds to mass parameter C of Fig. 11. This case was calculated to see whether the use of a smaller inertia would result in a more rapid response and thus to greater prompt fission. This is not the case. This fission probability increases and with it the prompt component; however the shape of the $P(t)$ curve changes very little. The curve labeled (E) results from the use of 200 $\hbar^2$/MeV for θ_1. This results in a reduction of the time-dependent rotation-vibration term in Eq. (4.4), which acts as an angular momentum barrier. The fission probability again increases. The shape of $P(t)$ changes slightly, but without a significant change in the prompt component. Curve (F) results from the use of a more fissile target, ^{250}Cm. The nucleus ^{250}Cm has a lower fission barrier than ^{238}U. Because of this, the fission yield in curve (F) is higher than that in curve (A); however, again the shape is the same, and one sees no evidence that more fissile nuclei undergo significantly more prompt fission.

ACKNOWLEDGMENTS

This research was supported in part by the Division of Basic Energy Sciences, U. S. Department of Energy, under Contract No. W-7405-eng-26 with Union Carbide Corporation, the National Science Foundation, the Bundesministerium für Forschung und Technologie, and by Gesellschaft für Schwerionenforschung. One of us (W. T. P.) gratefully acknowledges his indebtedness to the Alexander von Humboldt Stiftung for the Senior U. S. Scientist Award and to the Institut für Theoretische Physik of the Johann Wolfgang Goethe University for its hospitality.

*Permanent address: Vanderbilt University, Nashville, Tenn. 37235.

[1]E. Guth and L. Wilets, Phys. Rev. Lett. 16, 30 (1966).
[2]L. Wilets, E. Guth, and J. S. Tenn, Phys. Rev. 156, 1349 (1967).
[3]K. Beyer and A. Winther, Phys. Lett. 30B, 296 (1969); K. Beyer, A. Winther, and U. Smilansky, *Proceedings of the International Conference on Nuclear Reactions Induced by Heavy Ions, Heidelberg, Germany, 1969* (North-Holland, Amsterdam, 1970), p. 804.
[4]H. Holm and W. Greiner, Phys. Rev. Lett. 26, 1647 (1971); Nucl. Phys. A195, 333 (1972).
[5]V. Oberacker, G. Soff, and W. Greiner, J. Phys. G 3, L271 (1977).

[6]S. Levit and U. Smilansky, Nucl. Phys. A315, 205 (1979).
[7]H. Kruse, W. T. Pinkston, W. Greiner, and V. Oberacker, J. Phys. G 5, L105 (1979).
[8]V. Oberacker, W. Greiner, H. Kruse, and W. T. Pinkston, Phys. Rev. C 20, 1453 (1979).
[9]H. Backe, F. Weik, P. A. Butler, V. Metag, J. B. Wilhelmy, D. Habs, G. Himmele, and H. J. Specht, Phys. Rev. Lett. 43, 1077 (1979); H. Backe, P. A. Butler, V. Metag, J. B. Wilhelmy, D. Habs, G. Himmele, and H. J. Specht (unpublished).
[10]P. Colombani, P. A. Butler, I. Y. Lee, D. Cline, R. M. Diamond, F. S. Stephens, and D. Ward, Phys. Lett 65B, 39 (1976).
[11]P. A. Butler, I. Y. Lee, J. O. Newton, Y. ElMasri, M. M. Aleonard, P. Colombani, R. M. Diamond, F. S. Stephens, R. W. Lougheed, and E. K. Hulet, Phys. Lett. 68B, 122 (1977).
[12]D. Habs, V. Metag, J. Schukraft, H. J. Specht, C. O. Wene, and K. D. Hildenbrand, Z. Phys. A 283, 261 (1977).
[13]G. Franz, J. V. Kratz, W. Brüchle, H. Folger, and B. Haefner, Z. Phys. A 291, 167 (1979).
[14]V. Oberacker, H. Kruse, W. T. Pinkston, and W. Greiner, *Proceedings of the International Symposium on Continuum Spectra of Heavy Ion Reactions, San Antonio, Texas, 1979* (unpublished).
[15]Even though we shall not treat the imaginary potentials explicitly in this paper, we want to stress that they may play an important role in smearing out the interference minimum arising from Coulomb and nuclear excitation.
[16]K. Alder and A. Winther, *Electromagnetic Excitation—Theory of Coulomb Excitation with Heavy Ions* (North-Holland, Amsterdam, 1975).
[17]J. M. Eisenberg and W. Greiner, *Nuclear Theory* (North-Holland, Amsterdam, 1970), Vol. I.
[18]B. B. Back, O. Hansen, H. C. Britt, and J. D. Garrett, Phys. Rev. C 9, 1924 (1974).
[19]U. Fano, Phys. Rev. 124, 1866 (1961).
[20]M. W. Guidry, H. Massmann, R. Donangelo, and J. O. Rasmussen, Nucl. Phys. A274, 183 (1976).
[21]G. Ulfert, V. Metag, D. Habs, and H. J. Specht, Phys. Rev. Lett. 42, 1596 (1979).
[22]A. Mekjian, in *Advances in Nuclear Physics*, edited by M. Baranger and E. Vogt (Plenum, New York, 1973), Vol. 7.
[23]J. E. Lynn, United Kingdom Atomic Energy Research Establishment Report No. AERE-R5891, 1968 (unpublished).
[24]B. B. Back, Nucl. Phys. A228, 323 (1974).
[25]J. E. Lynn and B. B. Back, J. Phys. A 7, 395 (1974).
[26]P. D. Goldstone and P. Paul, Phys. Rev. C 18, 1733 (1978).
[27]M. Goerlach, D. Habs, M. Just, V. Metag, P. Paul, H. J. Specht, and H. J. Maier, Z. Phys. A 237, 171 (1978).
[28]H. C. Britt *et al.*, Phys. Rev. C 4, 1444 (1971).
[29]J. M. Blatt and V. F. Weisskopf, *Theoretical Nuclear Physics* (Wiley, New York, 1952).
[30]H. J. Specht, Rev. Mod. Phys. 46, 773 (1974).
[31]A. Sobiczewski, S. Bjørnholm, and K. Pomorski, Nucl. Phys. A202, 274 (1973).
[32]J. D. Cramer and J. R. Nix, Phys. Rev. C 2, 1048 (1970).
[33]R. Vandenbosch and J. R. Huizenga, *Nuclear Fission* (Academic, New York, 1973).
[34]W. Nörenberg and H. A. Weidenmüller, *Introduction to the Theory of Heavy-Ion Collisions, Lecture Notes in Physics* (Springer, Berlin-Heidelberg, 1976), Vol. 51.
[35]A. Gilbert and A. G. W. Cameron, Can. J. Phys. 43, 1446 (1965).
[36]A. Faessler, W. Greiner, and R. K. Sheline, Nucl. Phys. 70, 33 (1965).
[37]H. Kruse, Ph. D. thesis, Vanderbilt University, 1979 (unpublished).
[38]R. D. Richtmeyer, *Difference Methods for Initial Value Problems* (Interscience, New York, 1957).